Radiation patterns at the two resonant frequencies of the structure for each polarization are shown in Figures 17 and 18. Results are presented for E Plane and H Plane, respectively, at 4.84 and 5.66 GHz. These results illustrate the excellent sectoral properties of the antenna. In the vertical plane the radiation is directive with low side lobes, in the horizontal plane these figures present an interesting sectoral pattern of 60°.

6. CONCLUSION

This manuscript proposes an original application of MPRS-FSS materials to build bipolar dual-band sectoral antennas with several advantages.

MPRS-FSS structures and a patch fed by two probes were combined to realize bipolar dual-band capabilities. The study of MPRS-FSS structures showed us that their electromagnetic properties allow designing high gain antennas design.

This article has shown the possibility for MPRS-FSS antennas to radiate in vertical and horizontal polarization with a sectoral pattern in azimuth.

This antenna is an excellent candidate for several applications owing to its multiband properties. The proposed structure dispenses with the need for complex feeding mechanisms of patch array antennas.

REFERENCES

1. B. Lindmark and M. Nilsson, On the available diversity gain from different dual-polarized antennas, IEEE J Select Areas Commun 19 (2001), 287–294.
2. G.V. Trentini, Partially reflecting sheet arrays, IEEE Trans Antennas Propag 4 (1956), 666–671.
3. G.K. Palikaras, A.P. Feresidis, J.C Vardaxoglou, Cylindrical electromagnetic bandgap structures for directive base station antennas, IEEE Trans Antennas Propag 3 (2004), 87–89.
4. A.P. Feresidis and J.C. Vardaxoglou, High gain planar antenna using optimized partially reflective surfaces, IEE Proc Microwave Antennas Propag 148 (2001), 345–350.
5. M. Thevenot, C. Cheype, A. Reineix, and B. Jecko, Directive photonic bandgap antennas, IEEE Trans Microwave Theory Tech 47 (1999), 2115–2122.
6. C. Cheype, C. Serier, M. Thevenot, T. Monediere, A. Reineix, and B. Jecko, An electromagnetic bandgap resonator antenna, IEEE Trans Antennas Propag 50 (2002), 1285–1290.
7. D.R. Jackson and N.G. Alexopoulos, Gain enhancement methods for printed circuit antennas, IEEE Trans Antennas Propag 33 (1985), 976–987.
8. M. Qiu and S. He, High directivity patch antenna with both photonic bandgap substrate and photonic bangap cover, Microwave Opt Technol Lett 30 (2110), 41–44.
9. M. Hajj, H. Chreim, E. Rodes, E. Arnaud, D. Serhal, B. Jecko, Rectangular M-PRS structure for sectoral base station antenna with vertical polarization, Microwave Opt Technol Lett 52 (2010), 990.
10. Y.J. Lee, J. Yeo, R. Mittra, and W.S. Park, Design of a frequency selective surface (FSS) type superstrate for dual band directivity enhancement of microstrip patch antennas, IEEE AP-S International Symposium and USNC/URSI National Radio Science Meeting, Washington DC, July, 2005.
11. Y.J. Lee, J. Yeo, R. Mittra, and W.S. Park, Thin frequency selective surface (FSS) superstrate with different periodicities for dual-band directivity enhancement, IEEE International Workshop on Antenna Technology: Small Antennas and Novel Metamaterials (IWAT), March 2005, pp. 375–378.

WWAN/LTE PRINTED LOOP TABLET COMPUTER ANTENNA AND ITS BODY SAR ANALYSIS

Kin-Lu Wong,[1] Wan-Jhu Wei,[1] and Liang-Che Chou[2]
[1] Department of Electrical Engineering, National Sun Yat-Sen University, Kaohsiung 804, Taiwan; Corresponding author: vincent.chou@yageo.com
[2] Department of High Frequency Business, Yageo Corporation Nantze Branch, Kaohsiung 811, Taiwan

Received 27 February 2011

ABSTRACT: *A WWAN/LTE printed loop antenna for tablet computer application is presented. The printed loop antenna is a half-wavelength loop strip coupled-fed by a patch monopole, which performs not only as a coupling feed but also as an efficient radiator for the antenna. By embedding a printed distributed inductor in the loop strip, dual-resonance excitation of the half-wavelength mode of the coupled-fed loop antenna is obtained, which forms the antenna's lower band at about 800 MHz to cover the LTE700/GSM850/900 operation (704–960 MHz). The antenna's upper band is formed by both the resonant modes contributed by the patch monopole and the higher order resonant modes contributed by the loop strip. The upper band shows a large bandwidth (>1 GHz) to cover the GSM1800/1900/UMTS/LTE2300/2500 operation (1710–2690 MHz). Further, with a planar and compact structure (12 × 75 mm^2), the antenna is suitable to be disposed in the limited space inside the tablet computer and meets the body specific absorption rate (SAR) requirement (<1.6 W/kg for 1-g body tissue) for practical applications. Details of the proposed antenna and its body SAR results are presented.*
 Microwave Opt Technol Lett 53:2912–2919, 2011; View this article online at wileyonlinelibrary.com. DOI 10.1002/mop.26377

Key words: *mobile antennas; tablet computer antennas; WWAN antennas; LTE antennas; body SAR*

1. INTRODUCTION

The loop antennas have recently found promising applications in the mobile communication devices, especially in the mobile handset as internal antennas [1–14]. The internal loop antennas are attractive for mobile devices mainly because along the resonant path of the loop antenna there are generally no open ends with null currents, which is different from the traditional monopole or shorted monopole antennas [15–19]. In this case, the problem with strong near-field electric fields at the open end as occurred for the traditional monopole antennas can be avoided. The closed resonant path of the loop antenna can hence lead to smaller coupling effects between the antenna and nearby system ground plane of the mobile devices. Further, with the near-field electric field being weaker, the specific absorption rate (SAR) [20–22] values of the human tissue exposed to the antenna's radiation can be expected to be smaller. This feature makes the loop antenna attractive for practical applications in the handheld devices such as the handsets and tablet computers in which decreased near-field emission to achieve low head SAR or body SAR [23] values is demanded for the embedded internal antennas.

In this article, we demonstrate a promising printed loop antenna embedded with a distributed inductor for tablet computer applications. The antenna can cover the eight-band WWAN/LTE operation and meet the body SAR specification (SAR value for 1-g body tissue less than 1.6 W/kg) required for practical applications [24]. The antenna has a planar structure and is easy to be printed on an FR4 substrate at low cost. The printed loop strip is coupled-fed using a patch monopole which is

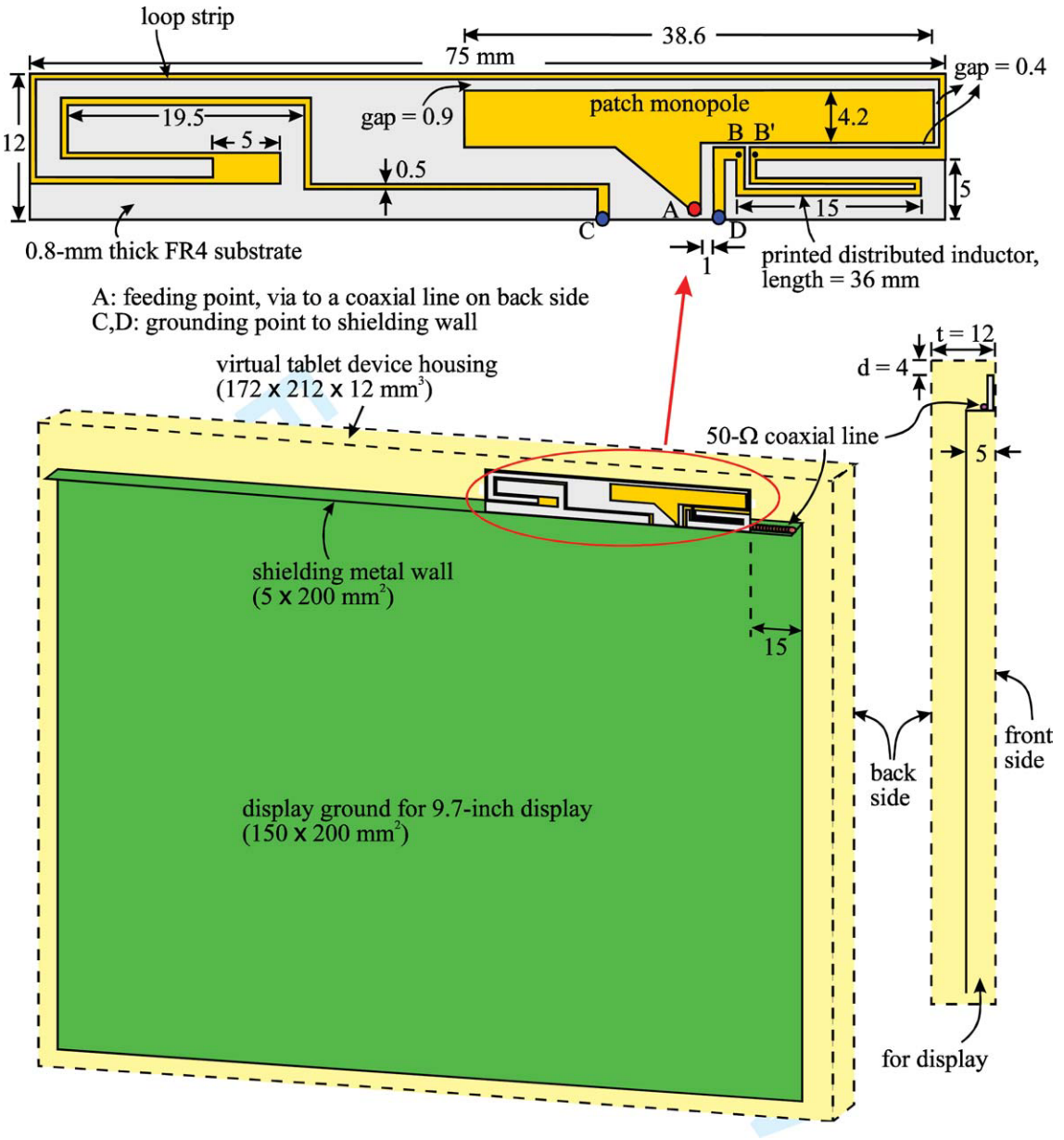

Figure 1 Geometry of the WWAN/LTE coupled-fed printed loop antenna embedded with a distributed inductor for tablet computer applications. [Color figure can be viewed in the online issue, which is available at wileyonlinelibrary.com]

encircled by the loop strip. Owing to the presence of the distributed inductor, whose effect is similar to that of a lumped chip inductor [23], a dual-resonant half-wavelength loop mode can be excited to cover the desired 704–960 MHz (704–787/824–894/880–960 MHz) band for the LTE700/GSM850/900 operation. Also, the patch monopole which performs as a coupling feed and an efficient radiator as well contributes resonant modes to combine with the higher order resonant modes of the coupled-fed loop strip to form a wide upper band for the antenna to cover the desired 1710–2690 MHz (1710–1880/1850–1990/1920–2170/2300–2400/2500–2690 MHz) band for the GSM1800/1900/UMTS/LTE2300/2500 operation. Operating principle of the proposed antenna is discussed in the article. Results of a fabricated prototype of the proposed antenna are also presented.

It is also noted that for the traditional laptop computers with a foldable two-section structure, their embedded internal antennas are generally mounted at the top edge of the display panel such that the antennas generally have a distance of larger than 20 cm to the user's body [25–28]. In this case, the body SAR is not required to be tested [24]. However, the tablet computers are generally of a one-section slate type and their internal antennas are to be mounted along the perimeter of the display panel. In this condition, the internal antennas are generally with a small distance of much less than 20 cm to the user's body in practical applications. Hence, the body SAR for the internal tablet computer antenna is required to be tested and should meet the limit of 1.6 W/kg for 1-g body tissue. The body SAR simulation models including the bottom face, landscape, and portrait conditions [24] for different orientations of the antenna to the flat phantom which contains tissue simulating liquid (TSL) [29] to simulate a portion of the user's body are described. The obtained body SAR results are analyzed.

2. PROPOSED ANTENNA

Figure 1 shows the geometry of the eight-band WWAN/LTE coupled-fed printed loop antenna with a distributed inductor for

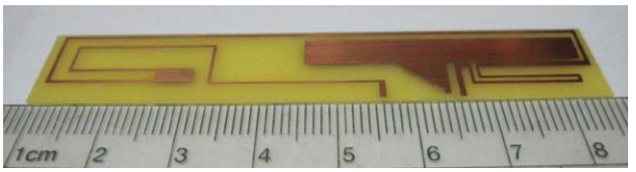

Figure 2 Photo of the fabricated antenna. [Color figure can be viewed in the online issue, which is available at wileyonlinelibrary.com]

tablet computer applications. In this study, the tablet computer or tablet device with a 9.7-in display is considered. The tablet computers with a similar display size as studied here have been commercially available. The antenna is printed on a 0.8-mm-thick FR4 substrate (relative permittivity, 4.4 and loss tangent, 0.02) of size 12×75 mm^2 and is mounted along the front edge of the shielding wall of the display panel such that a large distance between the antenna and the bottom surface of the computer housing shown by the dashed line in the figure can be obtained. Note that in this study the computer housing is a virtual housing only. The antenna is mounted at a distance of 12 mm (t) to the back side of the housing, and the distance to the top surface of the housing is 4 mm (d).

The shielding wall has a width of 5 mm and a length of 150 mm, which is generally added to provide some isolation between the internal antenna and the display, although it usually results in some degrading effects on the impedance matching of the internal antenna. By including the shielding metal wall in this study, the proposed antenna with a planar structure of 12×75 mm^2 on a 0.8-mm-thick FR4 substrate can still generate two wide operating bands to respectively cover the desired eight-band operation.

The display ground of size 150×200 mm^2 is for supporting the 9.7-in display of the tablet computer. The display is assumed to have a thickness of 5 mm and is disposed at the front side of the tablet computer. Also note that the antenna is placed close to one corner of the shielding wall with a distance of 15 mm, leaving large space along the shielding wall such that more possible internal antennas can be accommodated along the shielding wall.

The antenna mainly comprises a loop strip and a patch monopole encircled therein. Both the loop strip and patch monopole are efficient radiators, and the patch monopole also performs as a coupling feed to excite the loop strip through the coupling gaps shown in the figure. The front end (Point A) of the patch monopole is the feeding point of the antenna, which is connected through a via-hole in the FR4 substrate to a 50-Ω coaxial line along the shielding wall. The loop strip is bent to achieve a compact size and has a length of about 210 mm (excluding the Section BB', the distributed inductor), which is close to a half-wavelength at about 800 MHz. This makes the loop strip capable of generating a half-wavelength resonant mode in the desired lower band. However, it shows a narrow bandwidth and is far from covering the desired 704–960 MHz band. By further embedding a distributed inductor (Section BB', length about 35 mm and width 0.5 mm) whose effect is similar to the use of a chip inductor of 8.2 nH (Fig. 6 in Section 2), a dual-resonance excitation in the desired lower band is generated. This leads to a wide lower band obtained for the antenna to cover the desired 704–960 MHz band. This behavior is related to the excitation of a resonant mode showing very large peak resistance and reactance (Fig. 5 in Section 3), which is similar to a parallel resonant mode or antiresonant mode, at frequencies close to the original 0.5-wavelength loop mode at about 800 MHz. This greatly improves the impedance matching for frequencies at around 900 MHz or the high-frequency tail of the 0.5-wavelength loop mode, thus leading to significant bandwidth enhancement of the antenna's lower band.

In addition, the patch monopole alone can generate a wide operating band in the desired upper band, with the impedance matching close to 6-dB return loss or 3:1 VSWR, which is widely used design specification for the internal mobile device antennas for WWAN and LTE operation. By combing the higher order modes generated by the loop strip with the wide resonant mode contributed by the patch monopole, a very wide upper band of larger than 1 GHz can be obtained to cover the desired 1710–2690 MHz band. The proposed antenna can hence cover the eight-band operation of the WWAN and LTE systems.

3. RESULTS AND DISCUSSION

Figure 2 shows the photo of the fabricated antenna. The antenna is mounted at the shielding wall as shown in Figure 1 for testing. Figure 3 shows the measured and simulated return loss of the antenna. The simulated results are obtained using full-wave electromagnetic field simulation software HFSS version 12 [30]. The simulated results agree with the measured data. Two wide operating bands are obtained. The lower and upper bands can cover the desired 704–960 and 1710–2690 MHz bands with impedance matching better than the required 6-dB return loss (3:1 VSWR).

To analyze the effects of the patch monopole, the loop strip, and the embedded distributed inductor, Figure 4 shows the simulated return loss of the proposed antenna, the case with the patch monopole only (R1), and the case with the patch monopole and a simple loop strip (no printed distributed inductor; R2). For the R1 case, a wide band showing impedance matching close to 6-dB return loss in the desired upper band is seen. This can be seen more clearly in Figure 5 where the simulated input impedance of the three antennas studied in Figure 4 is shown. For the R1 case, there is a resonance at about 1920 MHz, and low variations in the input resistance are observed, which leads to the slow-varying return loss in the desired upper band seen in Figure 4.

For the R2 case, a narrow resonant mode at about 800 MHz is generated, which is a 0.5-wavelength loop mode contributed by the loop strip. The loop strip also contributes higher order resonant modes in the desired upper band to combine with the resonant mode contributed by the patch monopole. This leads to impedance matching enhancement in the desired upper band. When the distributed inductor is further embedded in the loop

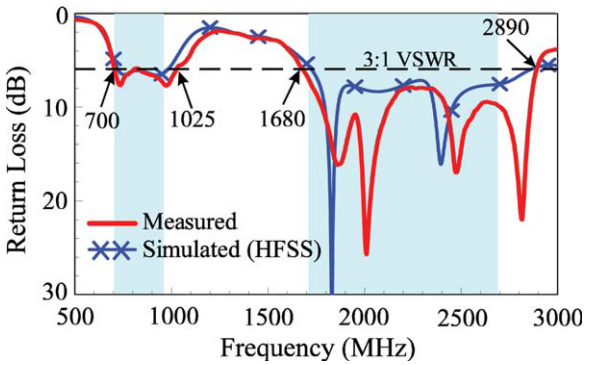

Figure 3 Measured and simulated return loss of the antenna. [Color figure can be viewed in the online issue, which is available at wileyonlinelibrary.com]

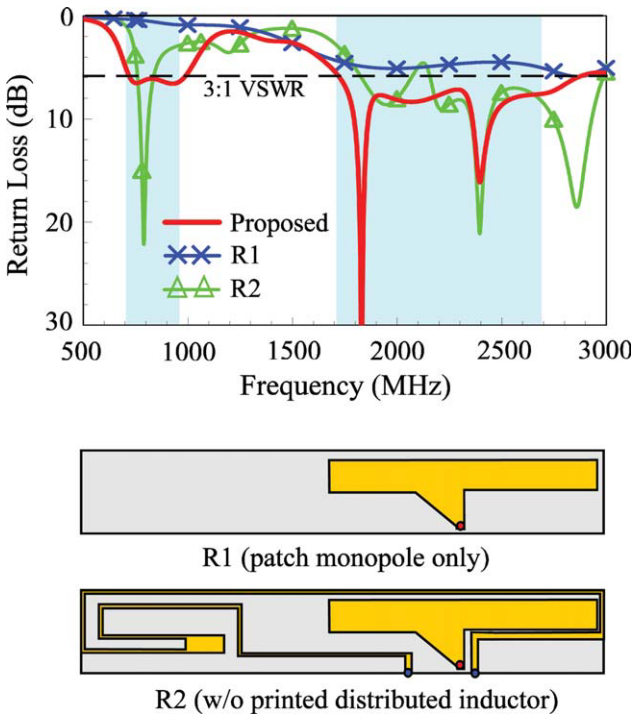

Figure 4 Simulated return loss (HFSS) of the proposed antenna, the case with the patch monopole only (R1), and the case with the patch monopole and a simple loop strip (no printed distributed inductor; R2). [Color figure can be viewed in the online issue, which is available at wileyonlinelibrary.com]

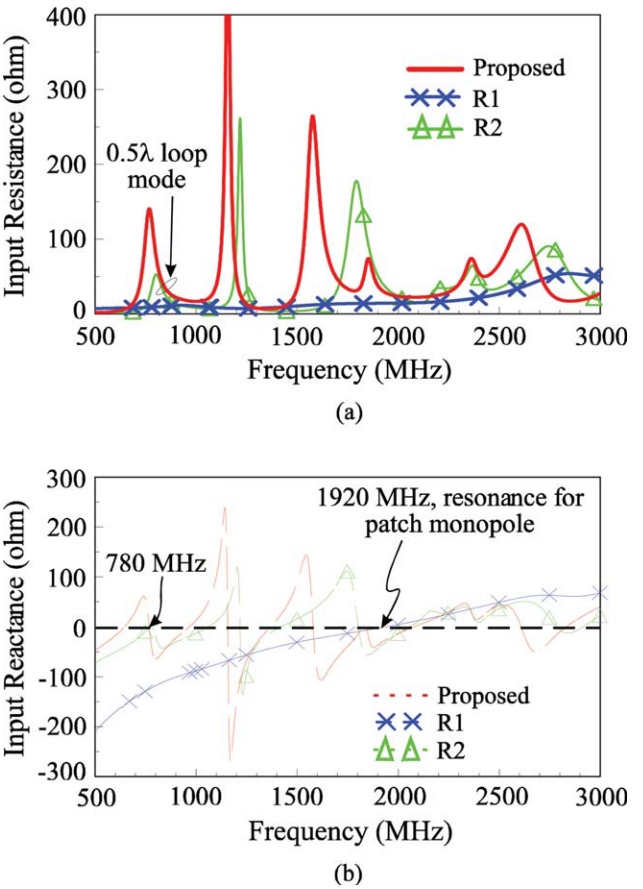

Figure 5 Simulated input impedance (HFSS) of the three antennas studied in Figure 4. (a) Input resistance. (b) Input reactance. [Color figure can be viewed in the online issue, which is available at wileyonlinelibrary.com]

strip, dual-resonance excitation in the desired lower band is obtained. From Figure 5, it can be seen that the obtained dual-resonance excitation is related to the excited resonant mode at about 1.15 GHz having very large peak resistance and reactance, which is similar to the characteristic of a parallel resonant mode or antiresonant mode. This resonant mode leads to increasing input resistance for frequencies at around 900 MHz or the high-frequency tail of the 0.5-wavelength loop mode, thereby resulting in a dual-resonance excitation and significant bandwidth enhancement in the desired lower band. Note that the parallel-resonance behavior of the excited resonant mode at about 1.15 GHz is probably related to the embedded distributed inductor which interacts with an equivalent capacitor formed in-between the patch monopole and the loop strip. In addition, with the embedded distributed inductor, further impedance matching enhancement is also obtained for frequencies in the desired upper band.

Figure 6 shows the simulated return loss of the proposed antenna and the case (R3) with a chip inductor of 8.2 nH replacing the printed distributed inductor (Section BB') in the loop strip. Other dimensions are the same as in Figure 1. From the obtained results, similar dual-resonance excitation is obtained for the proposed antenna and the R3 case. In the desired upper band, more resonant modes are also seen for the proposed antenna. This is largely because the distributed inductor also increases the total length of the loop strip, which leads to the excitation of more higher order loop resonant modes [23].

The radiation characteristics of the fabricated antenna are also studied. The antenna was tested with the display ground shown in Figure 1 and measured in a far-field anechoic chamber (ETS-Lindgren measurement system, http://www.ets-lindgren.com). Figure 7 shows the measured three-dimensional total-

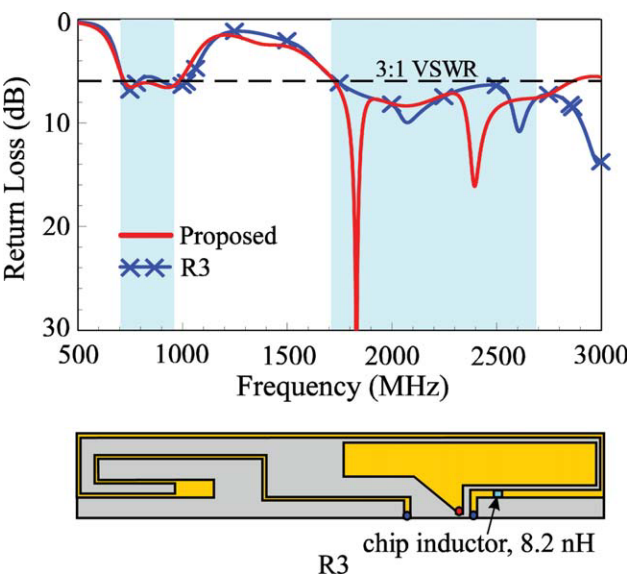

Figure 6 Simulated return loss (HFSS) of the proposed antenna and the case with a chip inductor of 8.2 nH replacing the printed distributed inductor (Section BB') in the loop strip. Other dimensions are the same as in Figure 1. [Color figure can be viewed in the online issue, which is available at wileyonlinelibrary.com]

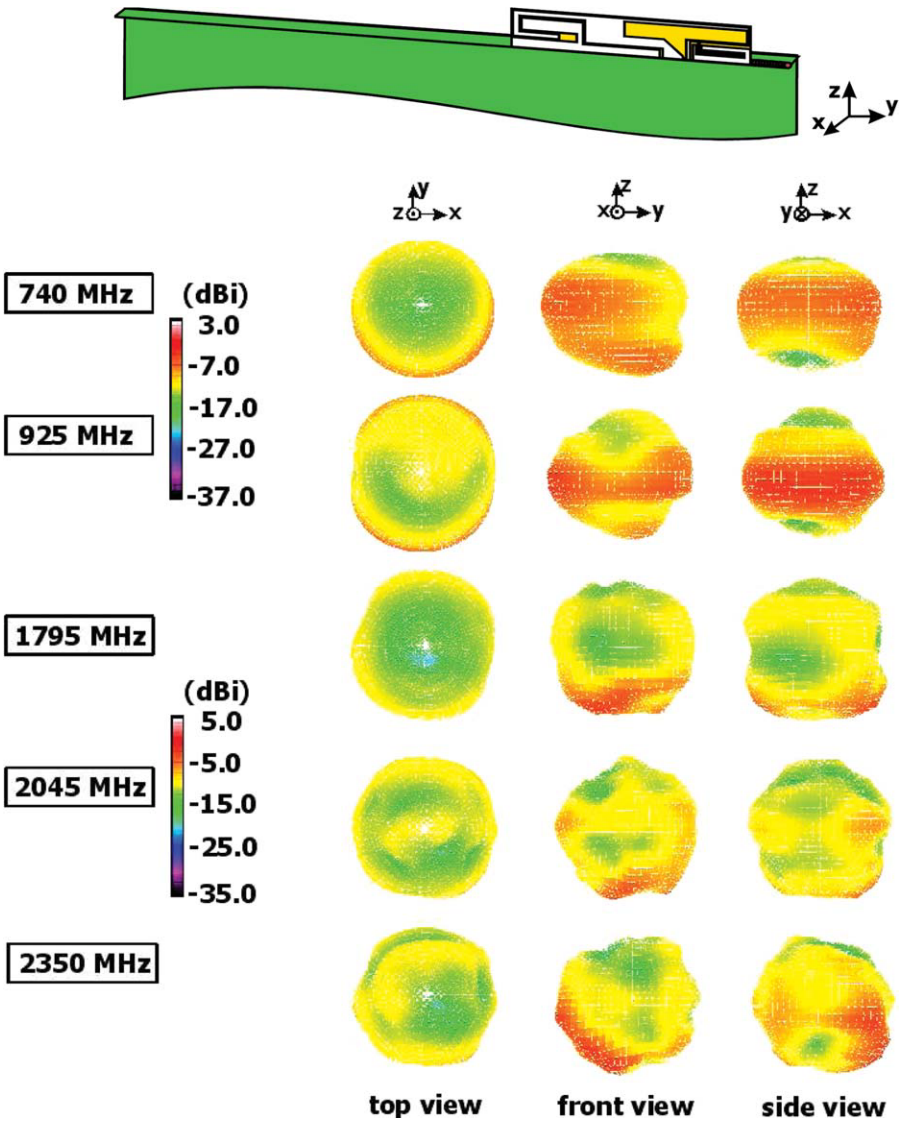

Figure 7 Measured three-dimensional total-power radiation patterns of the proposed antenna. [Color figure can be viewed in the online issue, which is available at wileyonlinelibrary.com]

power radiation patterns at typical frequencies. Three radiation patterns seen from the top, front, and side directions at each testing frequency are presented. At lower frequencies (740 and 925 MHz), the radiation patterns in the azimuthal plane (x–y plane) are close to omnidirectional. While at higher frequencies (1795, 2045, and 2350 MHz), some radiation dips in the azimuthal direction are seen. The obtained radiation patterns generally show no special distinctions to those of the reported internal WWAN antennas for the traditional laptop computers [31–34]. Figure 8 shows the measured antenna efficiency (mismatching loss included) for the antenna. The radiation efficiency is about 52–67 and 57–77% for the desired lower and upper bands, respectively. The efficiencies are all better than 50% for the eight operating bands.

The body SAR [24] is then tested for the antenna to meet the requirements for practical applications. Figure 9 shows the body SAR simulation model for the antenna based on the simulation software SEMCAD X version 14 [35]. In the simulation model, a flat phantom is used to simulate the human body. The flat phantom is formed by filling a 2-mm-thick plastic elliptic

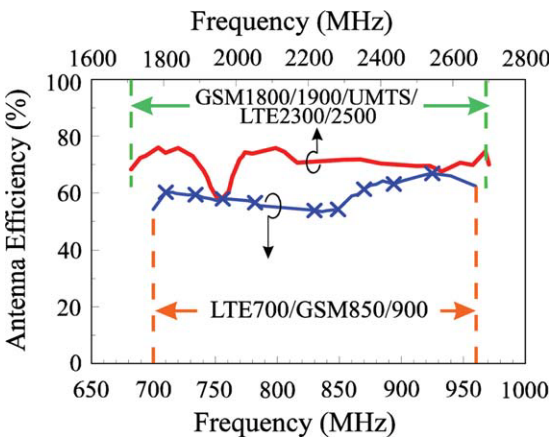

Figure 8 Measured antenna efficiency (mismatching loss included) of the antenna. [Color figure can be viewed in the online issue, which is available at wileyonlinelibrary.com]

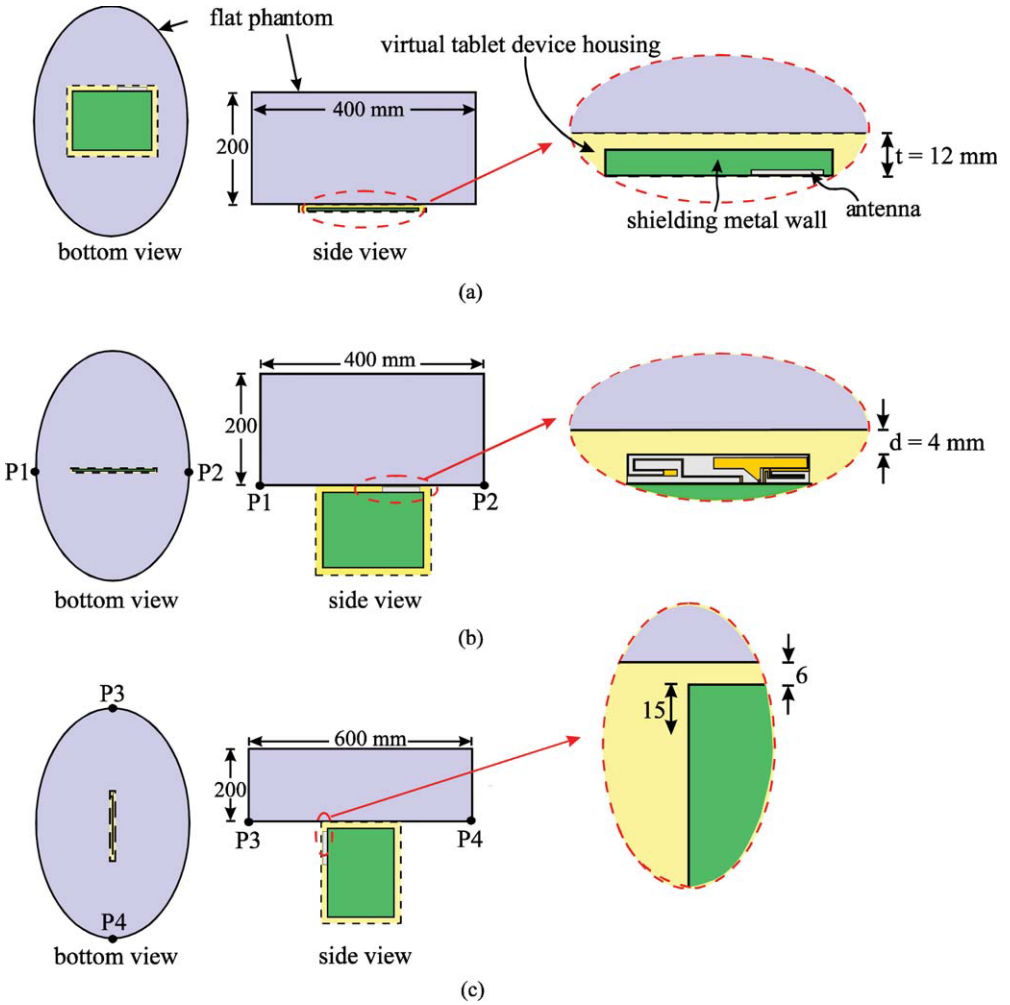

Figure 9 Body SAR simulation model for the proposed antenna. (a) Bottom face condition. (b) Primary landscape condition. (c) Primary portrait condition. [Color figure can be viewed in the online issue, which is available at wileyonlinelibrary.com]

cylindrical container with TSL [29]. The lengths of the longer and shorter axes of the container are 600 and 400 mm, respectively. The height of the container is 200 mm. According to the body SAR regulation [24], there are five conditions to be tested. The first one is the bottom face condition [Fig. 9(a)] in which the display is parallel to the flat phantom and the back surface of the computer housing is in direct contact against the flat phantom. The other four conditions are for the display oriented perpendicular to the flat phantom, including two landscape conditions and two portrait conditions. The landscape conditions further includes the primary landscape and secondary landscape conditions, while the portrait conditions also include the primary portrait and secondary portrait conditions. For the primary landscape and primary portrait conditions, the testing configurations are shown in Figures 9(b) and 9(c). For the secondary landscape condition, the antenna is at the edge away from the flat phantom. In this case, the antenna has a large distance (>100 mm) to the flat phantom, and the obtained body SAR values for 1-g tissue are expected to be much smaller than the limit of 1.6 W/kg. So is the case for the secondary portrait condition in which the antenna is at the corner away from the flat phantom and the obtained body SAR values are also expected to be much smaller than 1.6 W/kg. Hence, in this study, only the body SAR results for the bottom face, primary landscape, and primary portrait conditions shown in Figure 9 are tested.

Results of the simulated return loss obtained using SEMCAD X [35] for the antenna in free space and the antenna with the flat phantom in the bottom face, primary landscape, and primary portrait conditions are first presented in Figure 10. The simulated results for the antenna in free space are similar to the

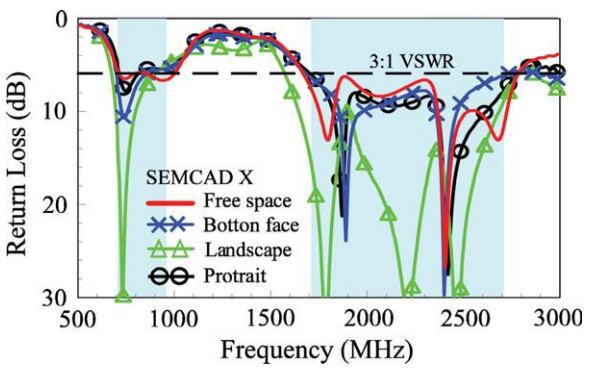

Figure 10 Comparison of the simulated return loss (SEMCAD X) for the antenna in free space and the antenna with the flat phantom in the bottom face, primary landscape, and primary portrait conditions. [Color figure can be viewed in the online issue, which is available at wileyonlinelibrary.com]

TABLE 1 Body SAR Results of the Antenna for 1-g Body Tissue; t = 12 mm and d = 4 mm

Frequency (MHz)	740	859	925	1795	1920	2045	2350	2595
Input power (W)	0.125	0.25	0.25	0.125	0.125	0.125	0.125	0.125
1-g SAR (W/kg)								
Bottom face	0.42	0.93	1.18	1.00	1.01	1.17	1.10	1.41
Prim. landscape	0.33	1.03	1.59	0.32	0.66	0.39	0.71	1.57
Prim. portrait	0.08	0.10	0.09	0.21	0.12	0.21	0.13	0.27
Return loss (dB)								
Bottom face	10.6	5.9	5.5	7.5	12.9	9.6	8.8	7.5
Prim. landscape	22.8	7.1	5.6	30.5	10.5	16.7	14.5	14.8
Prim. portrait	7.5	5.4	5.4	8.1	8.4	9.0	8.6	10.7
Free space	6.5	6.0	6.6	13.1	6.7	8.3	7.9	10.4

The return loss shows the impedance matching level of the antenna at each testing frequency.

TABLE 2 Body SAR Results of the Antenna as a Function of t for 1-g Body Tissue in the Bottom Face Condition; d = 4 mm

Frequency (MHz)	740	859	925	1795	1920	2045	2350	2595
1-g SAR (W/kg)								
t = 10 mm	0.56	1.24	1.58	1.52	1.47	1.71	1.63	2.18
t = 12 mm	0.42	0.93	1.18	1.00	1.01	1.17	1.10	1.41
t = 14 mm	0.33	0.72	0.91	0.67	0.68	0.84	0.79	0.87
Return loss (dB)								
t = 10 mm	10.4	5.8	5.4	7.5	8.7	9.4	8.8	7.5
t = 12 mm	10.6	5.9	5.5	7.5	12.9	9.6	8.8	7.5
t = 14 mm	10.7	6.0	5.5	7.5	11.5	9.9	9.1	7.6

corresponding results shown in Figure 3 using HFSS. Owing to the presence of the flat phantom, there are some variations in the impedance matching of the antenna. For the frequencies in the desired lower and upper bands, the return loss is still better than about 5 and 6 dB, respectively.

Table 1 lists the simulated SAR values for the antenna dimensions shown in Figure 1. Results obtained at the central frequencies of the eight operating bands are shown. The input power at each frequency is 0.25 W (24 dBm) at 859 and 925 MHz for GSM850/900 operation and 0.125 W (21 dBm) at 1795, 1920, 2045, 740, 2350, and 2595 MHz for GSM1800/1900, UMTS, and LTE operation. The SAR values for the all three conditions meet the limit of 1.6 W/kg. Also note that the SAR value for the primary portrait condition is the lowest among the three tested conditions and is much smaller than 1.6 W/kg. This is mainly because the antenna in the primary portrait condition has the largest distance to the flat phantom among the three tested conditions.

Effects of the SAR values as a function of the distance t in the bottom face condition and the distance d in the primary landscape condition are further analyzed. The results are listed in Tables 2 and 3. In Table 2, the SAR results for the distance t varied from 10 to 14 mm in the bottom face condition are presented. The body SAR values are increased with a decrease in the distance t. This is mainly owing to the antenna being closer to the flat phantom. For higher frequencies at 2045, 2350, and 2595 MHz for t = 10 mm, SAR values larger than 1.6 W/kg are also seen. As the distance t is also the thickness of the computer housing in this study, obtained results suggest that when the thickness of the tablet computer is larger than about 12 mm, the body SAR of the proposed antenna can meet the limit of 1.6 W/kg for practical applications.

Table 3 lists the SAR values for the distance d varied from 3 to 5 mm in the primary landscape condition. Other dimensions are the same as in Figure 1. For d = 5 mm, smaller SAR values are seen, which is reasonable because the antenna has a larger distance to the flat phantom. For d = 3 mm, increased SAR values are seen. At 925 and 2595 MHz, the SAR values are larger than 1.6 W/kg, exceeding the limit for practical applications. At other frequencies, the SAR values still meet the limit of 1.6 W/kg. Obtained results indicate that the values of d and t are important factors for the antenna to meet the body SAR limit for tablet computer applications.

4. CONCLUSION

A printed loop antenna promising for WWAN/LTE operation in the tablet computer has been proposed. The antenna has a

TABLE 3 Body SAR Results of the Antenna as a Function of d for 1-g Body Tissue in the Primary Landscape Condition; t = 12 mm

Frequency (MHz)	740	859	925	1795	1920	2045	2350	2595
1-g SAR (W/kg)								
d = 3 mm	0.37	1.18	1.85	0.41	0.72	0.43	0.78	1.79
d = 4 mm	0.33	1.03	1.59	0.32	0.66	0.39	0.71	1.57
d = 5 mm	0.29	0.89	1.37	0.26	0.57	0.35	0.62	1.38
Return loss (dB)								
d = 3 mm	18.9	7.6	6.2	31.5	11.8	17.3	14.5	14.7
d = 4 mm	22.8	7.1	5.6	30.5	10.5	16.7	14.5	14.8
d = 5 mm	28.8	6.8	5.1	29.6	9.0	15.9	14.5	14.9

uniplanar structure and can be printed on an FR4 substrate at low cost. The antenna is formed by a half-wavelength loop strip and a patch monopole encircled therein. A bandwidth enhancement technique of embedding a distributed inductor in the loop strip to achieve a dual-resonance excitation in the desired lower band to cover the LTE700/GSM850/900 operation has been shown. A wide upper band of larger than 1 GHz has also been obtained by the resonant modes contributed by the patch monopole and the higher order loop resonant modes contributed by the loop strip. The obtained upper band covers the GSM1800/1900/UMTS/LTE2300/2500 operation. The body SAR results of the proposed antenna have also been studied. Results indicate that the proposed antenna can meet the body SAR limit of 1.6 W/kg and is promising for practical WWAN/LTE tablet computer applications.

REFERENCES

1. R.L. Li, E.M. Tentzeris, J. Laskar, V.F. Fusco, and R. Cahill, Broadband loop antenna for DCS-1800/UMT-2000 mobile phone handsets, IEEE Microw Wirel Compon Lett 12 (2002), 305–307.
2. B.K. Yu, B. Jung, H.J. Lee, F.J. Harackiewwicz, and B. Lee, A folded and bent internal loop antenna for GSM/DCS/PCS operation of mobile handset applications, Microw Opt Technol Lett 48 (2006), 463–467.
3. B. Jung, H. Rhyu, Y.J. Lee, F.J. Harackiewwicz, M.J. Park, and B. Lee, Internal folded loop antenna with tuning notches for GSM/GPS/DCS/PCS mobile handset applications, Microw Opt Technol Lett 48 (2006), 1501–1504.
4. C.I. Lin and K.L. Wong, Internal meandered loop antenna for GSM/DCS/PCS multiband operation in a mobile phone with the user's hand, Microw Opt Technol Lett 49 (2007), 759–765.
5. Y.W. Chi and K.L. Wong, Internal compact dual-band printed loop antenna for mobile phone application, IEEE Trans Antennas Propag 55 (2007), 1457–1462.
6. C.I. Lin and K.L. Wong, Internal multiband loop antenna for GSM/DCS/PCS/UMTS operation in the small-size mobile phone, Microw Opt Technol Lett 50 (2008), 1279–1285.
7. K.L. Wong and C.H. Huang, Printed loop antenna with a perpendicular feed for penta-band mobile phone application, IEEE Trans Antennas Propag 56 (2008), 2138–2141.
8. Y.W. Chi and K.L. Wong, Half-wavelength loop strip fed by a printed monopole for penta-band mobile phone antenna, Microw Opt Technol Lett 50 (2008), 2549–2554.
9. Y.W. Chi and K.L. Wong, Compact multiband folded loop chip antenna for small-size mobile phone, IEEE Trans Antennas Propag 56 (2008), 3797–3803.
10. W.Y. Li and K.L. Wong, Seven-band surface-mount loop antenna with a capacitively coupled feed for mobile phone application, Microw Opt Technol Lett 51 (2009), 81–88.
11. Y.W. Chi and K.L. Wong, Very-small-size printed loop antenna for GSM/DCS/PCS/UMTS operation in the mobile phone, Microw Opt Technol Lett 51 (2009), 184–192.
12. Y.W. Chi and K.L. Wong, Very-small-size folded loop antenna with a band-stop matching circuit for WWAN operation in the mobile phone, Microw Opt Technol Lett 51 (2009), 808–814.
13. Y.W. Chi and K.L. Wong, Quarter-wavelength printed loop antenna with an internal printed matching circuit for GSM/DCS/PCS/UMTS operation in the mobile phone, IEEE Trans Antennas Propag 57 (2009), 2541–2547.
14. W.Y. Li and K.L. Wong, Small-size WWAN loop chip antenna for clamshell mobile phone with hearing-aid compatibility, Microw Opt Technol Lett 51 (2009), 2327–2335.
15. H. Kanj and S.M. Ali, Compact multiband folded 3-D monopole antenna, IEEE Antennas Wirel Propag Lett 8 (2009), 185–188.
16. A.R. Razali and M.E. Bialkowski, Coplanar inverted-F antenna with open-end ground slots for multiband operation, IEEE Antennas Propag Lett 8 (2009), 1029–1032.
17. C.L. Liu, Y.F. Lin, C.M. Liang, S.C. Pan, and H.M. Chen, Miniature internal penta-band monopole antenna for mobile phones, IEEE Trans Antennas Propag 58 (2010), 1008–1011.
18. K.L. Wong and S.C. Chen, Printed single-strip monopole using a chip inductor for penta-band WWAN operation in the mobile phone, IEEE Trans Antennas Propag 58 (2010), 1011–1014.
19. T.W. Kang and K.L. Wong, Chip-inductor-embedded small-size printed strip monopole for WWAN operation in the mobile phone, Microw Opt Technol Lett 51 (2009), 966–971.
20. American National Standards Institute (ANSI), Safety levels with respect to human exposure to radio frequency electromagnetic fields, 3 kHz to 300 GHz, ANSI/IEEE standard C95.1, American National Standards Institute, Boulder, CO, 1999.
21. IEC 62209-1, Human exposure to radio frequency fields from hand-held and body-mounted wireless communication devices—Human models, instrumentation, and procedures, Part 1: Procedure to determine the specific absorption rate (SAR) for hand-held devices used in close proximity to the ear (frequency range of 300 MHz to 3 GHz), IEC, 2005.
22. C.H. Li, E. Ofli, N. Chavannes, and N. Kuster, Effects of hand phantom on mobile phone antenna performance, IEEE Trans Antennas Propag 57 (2009), 2763–2770.
23. C.H. Chang and K.L. Wong, Small-size printed monopole with a printed distributed inductor for penta-band WWAN mobile phone application, Microw Opt Technol Lett 51 (2009), 2903–2908.
24. Federal Communications Commission, Office of Engineering and Technology, Mobile and Portable Device RF Exposure Equipment Authorization Procedures, OET/Lab Knowledge Database publication number 447498 item 7, Federal Communications Commission, 2007.
25. K.L. Wong and L.C. Lee, Multiband printed monopole slot antenna for WWAN operation in the laptop computer, IEEE Trans Antennas Propag 57 (2009), 324–330.
26. C.H. Chang and K.L. Wong, Internal coupled-fed shorted monopole antenna for GSM850/900/1800/1900/UMTS operation in the laptop computer, IEEE Trans Antennas Propag 56 (2008), 3600–3604.
27. X. Wang, W. Chen, and Z. Feng, Multiband antenna with parasitic branches for laptop applications, Electron Lett 43 (2007), 1012–1013.
28. C. Zhang, S. Yang, S. El-Ghazaly, A.E. Fathy, and V.K. Nair, A low-profile branched monopole laptop reconfigurable multiband antenna for wireless applications, IEEE Antennas Wirel Propag Lett 8 (2009), 216–219.
29. Tissue Simulating Liquid for SAR Measurement, NTT Advanced Technology Corporation. Available at: http://www.ntt-at.com/products_e/sar/index.html.
30. Available at: http://www.ansoft.com/products/hf/hfss/, ANSYS HFSS.
31. K.L. Wong and S.J. Liao, Uniplanar coupled-fed printed PIFA for WWAN operation in the laptop computer, Microw Opt Technol Lett 51 (2009), 549–554.
32. K.L. Wong and F.H. Chu, Internal planar WWAN laptop computer antenna using monopole slot elements, Microw Opt Technol Lett 51 (2009), 1274–1279.
33. T.W. Kang and K.L. Wong, Internal printed loop/monopole combo antenna for LTE/GSM/UMTS operation in the laptop computer, Microw Opt Technol Lett 52 (2010), 1673–1678.
34. K.L. Wong, W.J. Chen, L.C. Chou, and M.R. Hsu, Bandwidth enhancement of the small-size internal laptop computer antenna using a parasitic open slot for the penta-band WWAN operation, IEEE Trans Antennas Propag 58 (2010), 3431–3435.
35. SEMCAD, Schmid & Partner Engineering AG (SPEAG), Germany. Available at: http://www.semcad.com.